CHEMISTRY OF MATERIALS
Article

Chem. Mater. **2009,** *21,* 2817–2824 2817
DOI:10.1021/cm900490t

Design of $SiO_2-Al_2O_3-MoO_3$ Metathesis Catalysts by Nonhydrolytic Sol−Gel

Damien P. Debecker,[†] Karim Bouchmella,[‡] Claude Poleunis,[§] Pierre Eloy,[†] Patrick Bertrand,[§] Eric M. Gaigneaux,[†] and P. Hubert Mutin*,[‡]

[†]*Unité de catalyse et chimie des matériaux divisés, Université catholique de Louvain, Croix du Sud 2/17, B-1348 Louvain-la-Neuve, Belgium,* [‡]*Institut Charles Gerhardt Montpellier, UMR5253 CNRS-UM2-ENSCM-UM1, Chimie Moléculaire et Organisation du Solide, Université de Monpellier 2, cc1701, 34095 Montpellier cedex 5, France, and* [§]*Unité de physico-chimie et de physique des matériaux, Université catholique de Louvain, Croix du Sud 1, B-1348 Louvain-la-Neuve, Belgium*

Received February 18, 2009. Revised Manuscript Received May 19, 2009

MoO_3-based heterogeneous catalysts prepared by dispersion of Mo-oxide species on preformed supports are highly regarded candidates for industrial light olefin metathesis. An original approach for the elaboration of Mo-based catalysts is presented here. Mesoporous ternary Si/Al/Mo mixed oxides are prepared in one step by a nonhydrolytic sol−gel route in nonaqueous medium. Taking advantage of the migration of Mo species during the calcination, effective catalysts with very good textures and highly dispersed surface Mo species are obtained, as shown by XRD, XPS, and TOF-SIMS characterization. The presence of isolated Mo species is evidenced and these species are proposed to be the precursors to the active species in the metathesis of propene. These new materials compare well with catalysts prepared by classical wet impregnation of silica−alumina supports with ammonium heptamolybdate, eventually outperforming them at high Mo loading.

1. Introduction

Mixed oxides have a tremendous importance as catalysts and catalyst supports. Accordingly, the synthesis of mixed oxides by sol−gel processing has attracted considerable attention.[1−3] However, the direct sol−gel preparation of elaborate catalysts involving an active oxide phase dispersed at the surface of a mixed oxide support remains a challenge, explaining why such catalysts are usually prepared indirectly, for instance, by grafting or impregnation of preformed supports.[4,5]

Conventional sol−gel routes are based on the hydrolysis and condensation of molecular precursors, usually alkoxides. The very different reaction rates of metal and silicon precursors make the simultaneous control of the structure and texture of mixed oxide gels difficult. Thus, even for relatively simple binary oxides such as SiO_2-TiO_2, complicated experimental procedures are required to prepare homogeneous mesoporous materials, including prehydrolysis of the less reactive precursors or modification with chelating agents of the more reactive ones, and low-temperature extraction with supercritical CO_2 (aerogels).[6]

Conversely, nonhydrolytic routes[7] based on the reaction of chloride precursors with alkoxide precursors or diisopropyl ether were shown to provide an excellent control over the stoichiometry and the homogeneity of mixed oxide gels. Furthermore, because of the generally high degree of condensation of nonhydrolytic gels, mesoporous xerogels with high surface area and pore volumes can be obtained by simple evaporative drying, thus avoiding the supercritical drying step. Accordingly, these nonhydrolytic routes are attracting increasing attention for the preparation of mixed oxide catalysts.[8−15]

In this article, we wish to report the first direct nonhydrolytic sol−gel synthesis of $SiO_2-Al_2O_3-MoO_3$ olefin metathesis catalysts with well-controlled textures and structures and offering catalytic performances similar to that of catalysts prepared by wet impregnation of a

*Corresponding author. Tel.: 334 6714 3970. Fax: 334 6714 3852. E-mail: hubert.mutin@univ-montp2.fr.

(1) Baiker, A.; Grunwaldt, J.-D.; Mueller, C. A.; Schmid, L. *Chimia* **1998**, *52*, 517–524.
(2) Gonzalez, R. D.; Lopez, T.; Gomez, R. *Catal. Today* **1997**, *35*, 293–317.
(3) Livage, J. *Catal. Today* **1998**, *41*, 3–19.
(4) Meille, V. *Appl. Catal., A* **2006**, *315*, 1–17.
(5) Schwarz, J. A.; Contescu, C.; Contescu, A. *Chem. Rev.* **1995**, *95*, 477–510.
(6) Schneider, M.; Baiker, A. *Catal. Today* **1997**, *35*, 339–365.
(7) Vioux, A. *Chem. Mater.* **1997**, *9*, 2292–2299.
(8) Barbieri, F.; Cauzzi, D.; De Smet, F.; Devillers, M.; Moggi, P.; Predieri, G.; Ruiz, P. *Catal. Today* **2000**, *61*, 353–360.
(9) Caetano, B. L.; Rocha, L. A.; Molina, E.; Rocha, Z. N.; Ricci, G.; Calefi, P. S.; de Lima, O. J.; Mello, C.; Nassar, E. J.; Ciuffi, K. J. *Appl. Catal., A* **2006**, *311*, 122–134.
(10) Cojocariu, A. M.; Mutin, P. H.; Dumitriu, E.; Fajula, F. o.; Vioux, A.; Hulea, V. *Chem. Commun.* **2008**, 5357−5359.
(11) Lafond, V.; Mutin, P. H.; Vioux, A. *J. Mol. Catal. A: Chem.* **2002**, *182−183*, 81–88.
(12) Lorret, O.; Lafond, V.; Mutin, P. H.; Vioux, A. *Chem. Mater.* **2006**, *18*, 4707–4709.
(13) Moggi, P.; Devillers, M.; Ruiz, P.; Predieri, G.; Cauzzi, D.; Morselli, S.; Ligabue, O. *Catal. Today* **2003**, *81*, 77–85.
(14) Mutin, P. H.; Popa, A. F.; Vioux, A.; Delahay, G. r.; Coq, B. *Appl. Catal., B* **2006**, *69*, 49–57.
(15) Popa, A. F.; Mutin, P. H.; Vioux, A.; Delahay, G.; Coq, B. *Chem. Commun.* **2004**, 2214–2215.

Published on Web 06/10/2009

commercial silica−alumina support with ammonium heptamolybdate.

Olefin metathesis is a powerful tool for upgrading abundant alkenes into highly demanded ones.[16] Chauvin, Grubbs, and Schrock received the Nobel Prize in 2005 for the development of homogeneous catalytic systems. These systems are still receiving considerable interest to date, mainly in the field of organic synthesis or polymerization chemistry.[17−20] The discovery of the transalkylidenation reaction was, however, made with alumina-supported molybdenum oxide catalysts at Phillips Petroleum Co.[21] Since then, many industrial applications of the olefin metathesis reaction have been developed, as recently reviewed by Mol.[22] Ease of recovery and ease of product separation make heterogeneous catalysts highly indicated for high tonnage industrial conversion of light alkenes. The "Phillips Triolefin Process" was the first commercial production of propene through the metathesis of ethene and 2-butene. The "Shell higher olefin process" (SHOP) is another example of industrial application in which a supported molybdenum metathesis catalyst is used for the conversion of alkenes.

Classical catalyst preparation methods involve the impregnation of a Mo precursor onto a preformed support (silica, alumina, silica−alumina), followed by calcination. The catalytic performance of supported molybdenum oxide catalysts is influenced by the nature of the support and the high activity of catalysts supported on silica−alumina has been ascribed to the acidic character of the support.[23,24] However, even with elaborate impregnation methods, obtaining a molecular-scale dispersion of Mo surface species remains difficult.

Here, nonhydrolytic Si−Al−Mo materials with different MoO_3 loadings were obtained in one step by reaction of low-cost chloride precursors and diisopropyl ether. To enrich the catalyst surface in the active MoO_x species, our strategy was to take advantage of the migration of these species toward the surface during the calcination step (Scheme 1). Such a migration could be anticipated considering the low Tammann temperature of molybdenum oxide. The structure and the catalytic activity in the self-metathesis of propene of these sol−gel materials were compared to those of catalysts prepared by wet impregnation of a commercial silica−alumina support with ammonium heptamolybdate.[25]

Scheme 1. Schematic Representation of the Preparation of the Nonhydrolytic Sol−Gel Catalysts

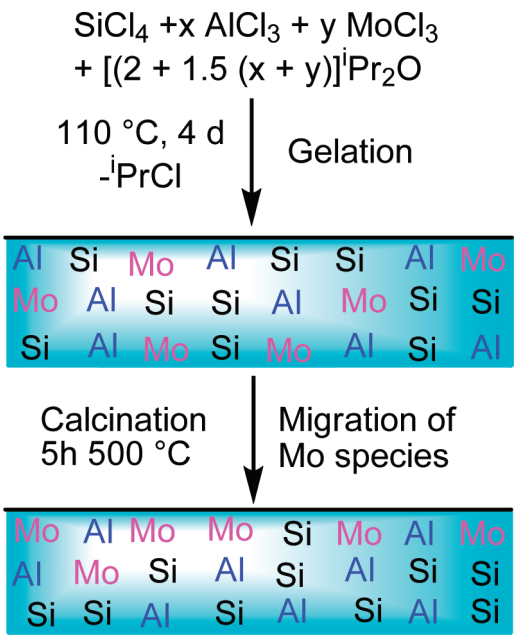

2. Experimental Section

2.1. Sample Preparation. *2.1.1. Sol−Gel Syntheses.* The nonhydrolytic sol−gel syntheses were performed under an argon atmosphere using a glovebox. $SiCl_4$ (Alfa Aesar 99.9%), $AlCl_3$ (Alfa Aesar 99.9%), and $MoCl_5$ (Alfa Aesar 99.6%) were used as received. $^iPr_2O$ (Aldrich 99%) was dried by distillation over sodium wire. The chloride precursors were introduced first in a 50 mL Pyrex glass tube, then the stoichiometric amount of $^iPr_2O$ and finally CH_2Cl_2 (see Supporting Information, Table S1). The solution obtained was frozen in liquid nitrogen under vacuum and the tube was sealed. The tube was heated in an oven at 383 K for 4 days under autogenous pressure (ca. 7 bar). After being cooled to room temperature, the tube was opened and the gel was crushed in a mortar and then dried at 393 K under vacuum (10 Pa) for 12 h. The xerogel was then calcined for 5 h at 773 K in air, leading to a pale yellowish powder.

2.1.2. Wet Impregnation. Reference catalysts were prepared by wet impregnation (WI) of a commercial silica−alumina support (Aldrich ; specific surface area 490 $m^2\ g^{-1}$; total pore volume 0.7 $cm^3\ g^{-1}$; weight ratio $SiO_2/Al_2O_3 = 7$). Prior to use, the support was calcined at 773 K for 15 h and stored at 383 K. Four grams of support was impregnated with 200 mL of a solution of ammonium heptamolybdate of appropriate concentration for 2 h under magnetic stirring. Water was then evaporated under reduced pressure in a rotavapor at 313 K. The recovered solid was dried at 383 K for 1 night and then calcined at 673 K for 2 h.

2.2. Characterization. N_2 physisorption experiments were performed at 77 K on a Micromeritics Tristar. The samples were outgassed at 473 K under vacuum (2 Pa). The pore size distribution was derived from the desorption branch using the BJH method; the micropore volume was estimated using *t*-plot analysis in the 3.5−5 Å range.

The weight percentages of Mo, Si, and Al were measured by inductively coupled plasma-atomic emission spectroscopy (ICP-AES) on an Iris Advantage apparatus from Jarrell Ash Corporation. The materials were dried at 378 K prior to measurements.

(16) Hoveyda, A.; Zhugralin, A. *Nature* **2007**, *450*, 243–251.
(17) Pariya, C.; Jayaprakash, K. N.; Sarkar, A. *Coord. Chem. Rev.* **1998**, *168*, 1–48.
(18) Schrock, R. R. *Angew. Chem., Int. Ed.* **2006**, *45*, 3748–3759.
(19) Poater, A.; Solans-Monfort, X.; Clot, E.; Coperet, C.; Eisenstein, O. *J. Am. Chem. Soc.* **2007**, *127*, 8207–8216.
(20) Malcolmson, S. J.; Meek, S. J.; Sattely, E. S.; Schrock, R. R.; Hoveyda, A. H. *Nature* **2008**, *456*, 933–937.
(21) Banks, R. L.; Bailey, G. C. *Ind. Eng. Chem. Prod. Res. Dev.* **1964**, *3*, 170–173.
(22) Mol, J. C. *J. Mol. Catal. A: Chem.* **2004**, *213*, 39–45.
(23) Aritani, H.; Fukuda, O.; Yamamoto, T.; Tanaka, T.; Imamura, S. *Chem. Lett.* **2000**, 66–67.
(24) Handzlik, J.; Ogonowski, J.; Stoch, J.; Mikolajczyk, M. *Catal. Lett.* **2005**, *101*, 65–69.
(25) Navez, D.; Weinberg, G.; Mestl, G.; Ruiz, P.; Gaigneaux, E. M. *Stud. Surf. Sci. Catal.* **2002**, *143*, 609–617.

TEM analyses were performed using a LEO922 electron microscope operating at 200KeV. The powdered samples, dispersed in 2-butanol, were deposited on copper grids coated with a porous carbon film and the solvent was then evaporated.

X-ray photoelectron spectroscopy (XPS) was performed on a Kratos Axis Ultra spectrometer (Kratos Analytical, Manchester, U.K.) equipped with a monochromatized aluminum X-ray source (powered at 10 mA and 15 kV). The pressure in the analysis chamber was about 1×10^{-6} Pa. The analyzed area was 700 μm $\times$ 300 μm. Charge stabilization was achieved by using the Kratos Axis device. The following sequence of spectra was recorded: survey spectrum, C1s, O1s, Si 2p, Al 2p, Mo 3d, Cl 2p, and C1s again to check for charge stability as a function of time and for the absence of degradation of the sample during the analyses. The binding energy (BE) values were referred to the C−(C, H) contribution of the C1s peak fixed at 284.8 eV. Further details on the experimental setup can be found in ref 26 and in the Supporting Information.

Positive and negative TOF-SIMS measurements were performed with a TOF-SIMS spectrometer from Charles Evans & Associates.[27] The sample was bombarded with pulsed Ga^+ ions (15 keV). The secondary ions were accelerated to $\pm$3 keV by applying a bias on the sample. The spreading of the initial energies of the secondary ions is compensated by deflection in three electrostatic analyzers. A postacceleration of 15 keV was applied at the detector entry. The analyzed area used in this work was a square of 120 $\times$ 120 μm, and the data acquisition time was 5 min. Charge effects were compensated by means of a pulsed electron flood gun (E_k=24 eV). The powders were pressed on a double-face silver tape. A stainless steel grid (non magnetic) was placed onto the sample surface in order to prevent variations of the surface potential. Relative intensities of Mo^+ ion were calculated by dividing the sum of the contribution of the three main isotopes of Mo (m/z = 92, 98, and 100) by the sum of all significantly contributions. The ions taken into consideration in this sum are H^+, CH_3^+, NH_4^+, Al^+, Si^+, $SiOH^+$, $^{92}Mo^+$, $^{98}Mo^+$, $^{100}Mo^+$, $^{92}MoO^+$, $^{98}MoO^+$, and $^{100}MoO^+$. Further details on this experimental setup can be found in ref *28* and in the Supporting Information.

NH_3-TPD profiles were obtained by using a Micromeritics AutoChem 2910 apparatus with a thermal conductivity detector. The samples were first activated in air flow at 723 K and NH_3 (5 vol% in He) was adsorbed at 373 K. After being purged with He for 2 h, NH_3 desorption was monitored as the sample was heated to 1073 K (heating rate of 10 K min^{-1}).

X-ray diffraction (XRD) measurements were performed on the fresh catalysts with a Siemens D5000 difractometer using the Kα radiation of Cu (λ = 1.5418 Å). The 2θ range was recorded between 5 and 75° at a rate of 0.02° s^{-1}. The ICDD-JCPDS database was used to identify the crystalline phases.

2.3. Catalytic Tests. All catalysts were sieved and selected in the 200−315 μm fraction. Catalytic tests were performed in a fixed-bed quartz reactor located inside an electrically heated oven. The catalytic bed was composed of (i) 200 mg of catalyst prepared by wet-impregnation diluted in 1 g of inert quartz spheres or (ii) 100 mg of catalyst prepared by sol−gel diluted in 500 mg of quartz spheres, in order to keep the volume of the catalytic bed approximately constant. The reactor was first purged under a 130 mL/min flow of pure He (Praxair. 99.995%) at room temperature for 30 min. The flow was then reduced to 60 mL/min and reactor was heated to 423 K for 150 min. Activation of the catalyst was then performed at 823 K for 150 min. After the sample was cooled under He to the reaction temperature (313 K), a 8 mL/min flow of pure propene (Praxair. 99.5%) was admitted. Both He and propene gases were purified with oxygen and moisture gas filters (Varian). These conditions were chosen in order to keep the conversion moderate (below 15%) and ensure that propene is supplied in excess along the catalytic bed.

Analysis of reactants and products was continuously performed by online gas chromatography (GC). The CP-3800 gas chromatography apparatus from Varian was used to quantify propene, ethene, and *cis*- and *trans*-butene and to detect the presence of other hydrocarbons and O_2, CO_2, and CO. The apparatus was equipped with one packed Hayesep Q column and one packed Molsieve 5A column both connected to a TCD detector and with one capillary AT alumina column (50 m $\times$ 0.53 mm) connected to a FID detector. He was used as carrier gas. The analysis parameters were set as to allow one analysis each 21 min. Conversion is calculated on the basis of the addition of the three metathesis products (ethene and *cis*- and *trans*-butene).

3. Results

3.1. Synthesis of the Materials. For this study, SiO_2−Al_2O_3−MoO_3 mixed oxides with different compositions were prepared by a one-step nonhydrolytic sol−gel route, involving the reaction at 313 K under autogenous pressure of $SiCl_4$, $AlCl_3$, and $MoCl_5$ precursors with $^iPr_2O$ in CH_2Cl_2. The amounts of precursors and reactants involved in the preparation of each sol−gel catalysts can be found in the Supporting Information, Table S1. The gels obtained were dried under vacuum then calcined for 5 h at 773 K in dry air. These samples are labeled SGx, where x is the nominal MoO_3 weight loading.

For comparison, MoO_3/SiO_2−Al_2O_3 catalysts with different MoO_3 loadings were prepared by wet impregnation (WI) of a commercial SiO_2−Al_2O_3 support with ammonium heptamolybdate. The materials are labeled WIx, where x represents the nominal MoO_3 weight loading. The SiO_2/Al_2O_3 weight ratios and MoO_3 loadings of both sol−gel and wet-impregnated samples derived from ICP-AES measurements are reported in Table 1.

3.2. Materials Characterization. All the sol−gel samples were mesoporous, with N_2 adsorption−desorption isotherms of type IV, according to the BDDT classification (Figure 1a). The sol−gel samples had specific surface areas ranging between 470 to 500 m^2 g^{-1} and average pore diameters ranging between 7.2 and 13.3 nm (Table 1). *t*-Plot analysis indicated that the surface area developed by micropore walls was very low. The texture of the SG samples compared well with that of the WI samples, which had slightly lower specific surface areas and significantly smaller pore diameters, around 5 nm (Figure 1b).

Transmission electron microscopy (TEM) gave an interesting picture of the morphology of the sol−gel samples: images of the SG10 sample showed the presence of porous particles in the 200−1000 nm range, with

(26) Debecker, D. P.; Faure, C.; Meyre, M. E.; Derre, A.; Gaigneaux, E. M. *Small* **2008**, *4*, 1806–1812.
(27) Rodriguez-Gonzalez, L.; Hermes, F.; Bertmer, M.; Rodriguez-Castellon, E.; Jimenez-Lopez, A.; Simon, U. *Appl. Catal., A* **2007**, *328*, 174–182.

Table 1. Composition and Texture of the Sol-Gel and Wet Impregnation Catalysts[a]

sample	MoO_3 wt % exp (th[b])	SiO_2/Al_2O_3	S_{BET} ($m^2\ g^{-1}$)	V_P ($cm^3\ g^{-1}$)	$S\mu$ ($m^2\ g^{-1}$)	D_P[d] (nm)
SG5	4.6 (4.4)	17	500	0.9	40	7.2
SG10	9.4 (10.6)	20	480	1.6	20	13.1
SG15	15.2 (14.4)	17	470	1.6	0	13.3
SG20	18.5 (19.8)	18	470	1.6	10	13.3
WI4	3.4 (4.0)	7[c]	440	0.7	0	4.8
WI8	7.9 (8.0)	7[c]	400	0.6	0	5.7
WI11	11.3 (11.0)	7[c]	400	0.6	0	4.4
WI17	17.1 (17.0)	7[c]	370	0.5	0	4.4

[a] Experimental MoO_3 loading and SiO_2/Al_2O_3 weight ratio of the materials are calculated from ICP AES results. Texture was measured by N_2-physisorption. [b] Nominal weight percentages calculated from the amount of reactants involved in the synthesis. [c] According to the manufacturer. [d] Average pore diameter ($4\ V_P/S_{BET}$).

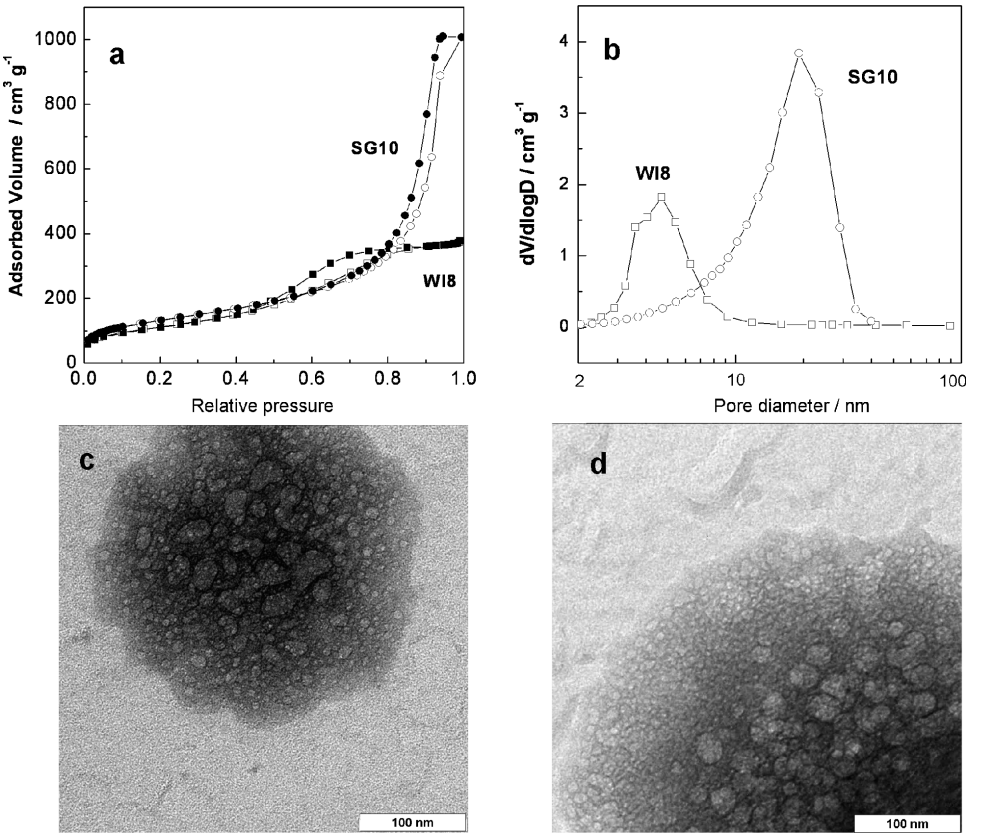

Figure 1. Texture of the catalysts. (a) N_2 adsorption−desorption isotherms at 77 K for SG10 and WI8 samples (open and filled symbols correspond to the adsorption and desorption branches, respectively); (b) pore size distributions derived from the desorption branches, using the BJH method; (c) TEM micrograph of a particle of the SG10 catalyst (scale bar = 100 nm) and (d) TEM image of a particle of the silica−alumina used as support for the WI catalyst (scale bar = 100 nm).

mesopores in the 2−15 nm range (Figure 1c). The silica−alumina support (Figure 1d) and the WI samples prepared from it appeared very similar, but with a higher proportion of small pores. These images were thus consistent with N_2-physisorption measurements.

The catalytic activity of supported molybdenum oxide catalysts is influenced by the nature of the support, and the high activity of catalysts supported on silica−alumina has been ascribed to the acidic character of the support, associated with the presence of protonated oxygen in Si−O−Al bridges ("bridging hydroxyl").[24] We used temperature-programmed desorption of ammonia (NH_3-TPD) to probe the acidity of the sol−gel samples (Figure 2). The thermogram obtained for a sample containing only Mo and Si oxides showed a broad desorption profile between 400 and 590 K, indicating the presence of weak acidic sites. The thermograms of all Al-containing samples showed that ammonia desorbed up to 723 K, indicating the presence of more acidic sites, intermediate between the weakly acidic sites on silica and the highly acidic sites found in zeolites.[27]

The XRD patterns of the different sol−gel samples presented in all cases a broad band around 20−25° typical of amorphous solids (Figure 3). There was no evidence of crystalline molybdenum oxide in the patterns of the sol−gel samples, showing that no MoO_3 crystallites larger than the detection limit − about 5 nm − were present. The only exception concerned the sample with the highest MoO_3 loading (SG20) for which a small diffraction line at 27.5° indicated the presence of traces of crystalline MoO_3

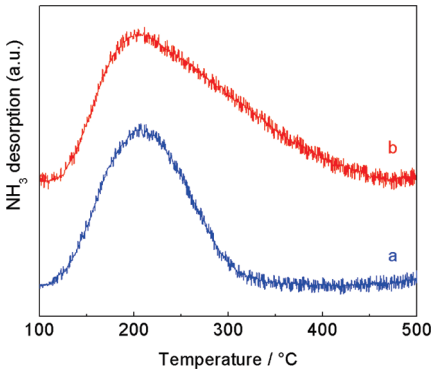

Figure 2. Acidity of the sol−gel samples as probed by temperature programmed desorption of ammonia (NH_3-TPD) on (a) a SG sample containing only SiO_2 and MoO_3 (10 wt %) and (b) SG10 sample.

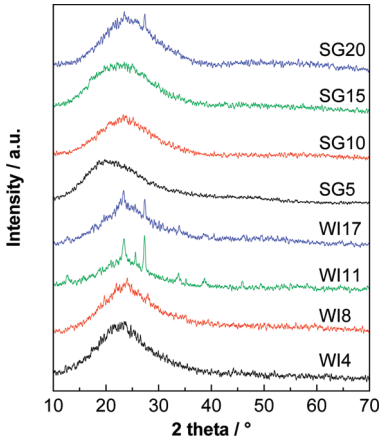

Figure 3. XRD diffractograms of SG*x* and WI*x* samples.

(JCPDS 05−0508). On the other hand, MoO_3 crystallites could clearly be detected in all the samples prepared by wet impregnation, with the exception of the one with the lowest MoO_3 loading, WI4.

The surface composition of the different samples was studied by XPS (Table 2). In addition, the effect of calcination was investigated for the sol−gel samples. The high amount of carbon and the significant amount of chlorine found on the fresh xerogels has to be related to the presence of residual O^iPr and Cl groups (inherent to the nonhydrolytic route used) at the surface of the xerogels. After calcination the carbon content decreased to about 5 at%, and chlorine was no more detected. The residual carbon content resulted from atmospheric carbon contamination and was similar for all calcined samples, regardless of their preparation method: sol−gel or impregnation.

The mixed oxide xerogels obtained by nonhydrolytic condensation reactions are generally described as highly homogeneous.[7] However, in order to obtain an active Mo-based catalyst, a high proportion of the Mo atoms should be present at the surface of the catalyst, so that they are accessible for the gaseous reactants. Our strategy was to apply an appropriate calcination treatment that would presumably result in the migration of Mo species toward the surface of the catalysts. As shown in Table 2, the surface Mo content of the calcined samples was significantly higher than in the fresh xerogels.

To verify that this increase was not due to the decrease in the C content, we plotted the Mo/(Si + Al + Mo) ratio as a function of the MoO_3 loading determined by ICP-AES (Figure 4a). This ratio was significantly higher for the calcined samples than for the fresh xerogels (with an exception for the catalyst containing only 5% of MoO_3). For a given MoO_3 loading, the surface concentrations of Mo on the calcined sol−gel samples were almost at the same level as on the samples obtained by wet impregnation, as shown in Figure 4a. This last observation can also be made concerning the outermost surface of the catalysts, as characterized with time-of-flight secondary ion mass spectroscopy (TOF-SIMS):[28] as shown in Figure 4b, the intensities of Mo^+ ions detected on WI and SG catalysts were similar.

Further insight on the Mo chemical environment might be gained from the position and width of the XPS Mo 3d peaks. The Mo 3d peak of fresh xerogels showed that two different oxidation states coexist: although the precursor is based on Mo^{5+}, it is reasonable to think that partial oxidation to Mo^{6+} occurs when the xerogel is exposed to air. The calcination step results in the production of fully oxidized Mo species characterized by a well-defined doublet. Table 2 shows that the Mo 3d binding energy (BE) is systematically higher in SG samples than in WI samples, suggesting that Mo^{6+} cations are located in different chemical environments in SG and in WI samples. However, it is difficult to draw further conclusions from this shift because the silica−alumina matrix that interacts with Mo atoms is different in both cases (different Si/Al ratio). The full width at half-maximum is higher for calcined SG samples than for WI samples, suggesting that the environment of Mo atoms is more variable in SG catalysts.

The TOF-SIMS general spectra of WI and SG catalysts were different (Figure 5). Typical patterns related to fragments containing one Mo atom are found for all WI and SG samples (peaks around 114, 129, 145, and 160 are attributed to MoO^-, MoO_2^-, MoO_3^-, and MoO_4^- respectively). On the other hand, clusters containing more than one Mo atom (patterns around 288, 305, and 432 are identified as the $Mo_2O_6^-$, $Mo_2O_7^-$, and $Mo_3O_9^-$, respectively) are detected for the WI8, WI11, and WI17 samples but never for SG samples, even at the highest loading. The detection of these clusters indicates the occurrence of Mo oxide oligomers or crystallites at the surface of the WI catalyst, whereas their absence in the case of SG sample indicates the occurrence of isolated Mo oxide surface species.

3.3. Activity Measurements. The cross-metathesis of butene and ethene to obtain highly demanded propene is an economically attractive process.[29] The reverse reaction − self-metathesis of propene − is usually studied for the purpose of fundamental research. The activity of the

(28) Bertrand, P.; Weng, L. T. *Mikrochim. Acta* **1996**, *13*, 167–182.
(29) Li, X.; Zhang, W.; Liu, S.; Xu, L.; Han, X.; Bao, X. *J. Catal.* **2007**, *250*, 55–66.

Table 2. Surface Characterization by X-ray Photoelectron Spectroscopy (XPS) on the Fresh and Calcined Sol−Gel Samples and the Wet-Impregnation Samples

	Si (at %)	Al (at %)	Mo (at %)	O (at %)	C (at %)	Cl (at %)	Mo $3d_{3/2}$ BE (eV)	Mo $3d_{3/2}$ fwhm (eV)
SG5 fresh	26.4	1.3	0.3	57.4	14.2	0.4	232.8[a]	3.1[a]
SG10 fresh	22.9	1.2	0.5	54.3	19.9	1.2	232.4[a]	2.5[a]
SG15 fresh	22.9	1.5	1.0	52.0	19.9	2.7	232.3[a]	2.4[a]
SG20 fresh	21.2	1.3	1.4	47.5	26.5	2.1	232.4[a]	2.7[a]
SG5	29.7	1.6	0.4	62.9	5.4	<0.1	233.1	3.0
SG10	27.1	2.3	1.0	64.6	5.1	<0.1	233.1	2.6
SG15	27.2	1.6	1.6	64.1	5.4	<0.1	233.1	2.4
SG20	26.4	1.6	2.0	64.4	5.6	<0.1	233.1	2.3
WI4	25.5	4.2	0.3	61.7	8.4	<0.1	232.6	2.2
WI8	25.6	4.1	0.8	63.3	6.3	<0.1	232.6	2.0
WI11	24.2	3.9	1.3	61.8	8.7	<0.1	232.6	1.8
WI17	24.5	4.2	1.9	60.1	9.3	<0.1	232.7	1.7

[a] Data given for the most oxidized (Mo^{6+}) component of the Mo 3d peak.

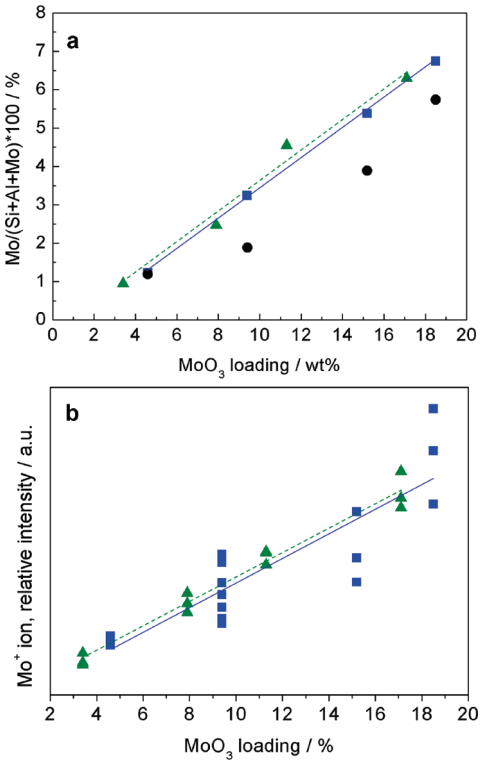

Figure 4. Surface characterization of the WI and SG catalysts by XPS and TOF-SIMS. (a) Mo/(Mo + Si + Al) XPS atomic concentration ratios as a function of the MoO_3 experimental weight loading for (■, plain interpolation line) calcined sol−gel catalysts; (●) fresh xerogel; and (▲, dotted interpolation line) catalysts prepared by wet impregnation. (b) Relative intensity of the Mo^+ ion detected in TOF-SIMS on (■) calcined sol−gel catalysts (plain interpolation line) and (▲) catalysts prepared by wet impregnation (dotted interpolation line). At least three measurements have been performed on each catalyst. The poorer reproducibility of the measure on the SG sample was ascribed to the more open porosity and more irregular surface of these samples.

WI and SG catalysts in the self-metathesis of propene has been tested at 313 K, after appropriate thermal activation (see the Experimental Section), under pure propene flow at atmospheric pressure. The reaction conditions were chosen in order to keep the conversion moderate (below 15%) and ensure that propene was supplied in excess along the catalytic bed. Under these conditions, byproducts were detected only as traces and the selectivity to metathesis products (ethene and *cis*- and *trans*-butene) was close to 100%.

The evolution of the conversion during catalytic tests with SG and WI samples are presented as Supporting Information. Sol−gel and impregnation catalysts behaved similarly: the activity first increased, reaching a maximum after 30−40 min, and then a progressive deactivation occurred. To compare the activity of SG and WI catalysts, it is necessary to take into account the mass of catalyst used in the reaction (100 mg for the SG*x* catalysts, 200 mg for the WI*x* catalysts). The specific activity of SG*x* and WI*x* catalysts (taken at 30 min on stream) was plotted as a function of the experimental MoO_3 weight loading (Figure 6). At low MoO_3 loading (up to 8 wt %), the specific activity of the WI catalysts was significantly higher than that of SG catalysts. At higher MoO_3 loadings (above 8 wt %), the specific activity of the WI catalysts remained constant. On the other hand, the maximum specific activity of the SG catalysts increased continuously with the MoO_3 loading and the specific activity of the SG20 catalyst was significantly higher than that of the best WI catalyst.

4. Discussion

The new strategy for designing active catalysts that is presented here differs greatly from classical preparation methods: instead of depositing a catalytically active phase on a preformed support, the active phase is first homogeneously incorporated with the other components of the catalyst and subsequently brought toward the surface of the material. Three main challenges need to be addressed in order to make this approach relevant: (i) all requirements related to the use of these materials as solid catalysts (good texture, control on the composition) have to be met; (ii) the active component should be available for the reactants at the surface of the catalyst; and (iii) the active species should be present in their most active form.

4.1. Control of Composition and Texture. As far as light olefin metathesis is concerned, formulations involving three different oxides (Mo, Si, and Al) are highly recommended.[30] The need for acidity of the metathesis catalysts is a well-known fact and we also show that introducing alumina in our systems results in an increase in acidity.

(30) Li, X.; Zhang, W.; Liu, S.; Xu, L.; Han, X.; Bao, X. *J. Phys. Chem. C* **2008**, *112*, 5955–5960.

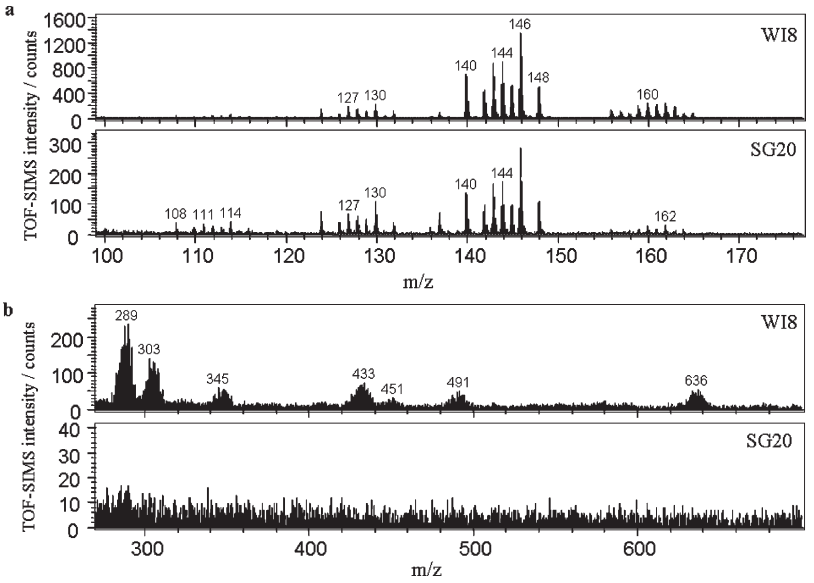

Figure 5. Parts of the negative TOF-SIMS spectra obtained with WI8 and SG20 catalysts. (a) From 99 to 177 *m*/*z*. (b) From 270 to 700 *m*/*z*. Each spectrum has been recorded at least three times. The relative intensities of every peak were always in good agreement. The same results have also been obtained after a repeated experiment performed 6 months after the main data acquisition campaign.

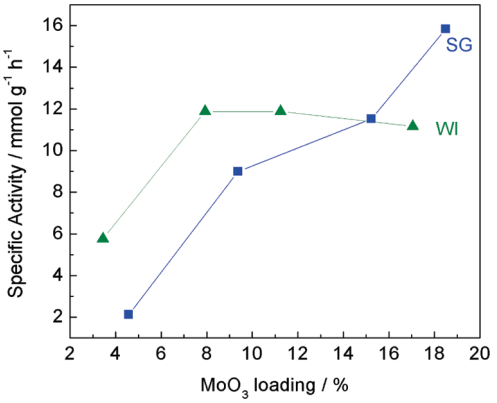

Figure 6. Maximum specific activity (expressed as mmol of propene converted per g of catalyst per h) measured after 30 min on stream with (■) catalysts prepared by sol−gel and (▲) catalysts prepared by wet impregnation.

The difficulty to design ternary mixed oxides including silica and a transition metal oxide with classical sol−gel technology (related to the very different reaction rates of silicon and metal precursors) is solved by using nonhydrolytic sol−gel chemistry. The good agreement between experimental and nominal compositions shows that the nonhydrolytic route used offers an excellent control over the composition of the materials. Moreover, nonhydrolytic sol−gel also provides an excellent control over the texture of the materials, which are mesoporous with high surface areas and pore volumes. TEM images show the presence of open pores, consistent with N_2-physisorption measurements. A first attempt to prepare ternary mixed oxides (Si−Al−Co) by a two-step nonhydrolytic sol−gel process has already been reported, but the texture of the materials (53 $m^2\ g^{-1}$ and 0.05 $cm^3\ g^{-1}$ after calcination at 673 K) was much less interesting.[9]

4.2. Migration of the Mo Species. The second challenge is to ensure that a high proportion of the active component involved in the preparation effectively has the opportunity to take part in the catalytic reaction. Our results show that the strategy used to provoke the migration of the Mo species toward the surface was successful. This phenomenon was anticipated considering the low Tammann temperature of MoO_3 (534 K). The migration of V oxide species with similar Tammann temperature (482 K) has been already observed during the calcination of V_2O_5−TiO_2 catalysts prepared by sol−gel.[14,31] The high temperature used in the calcination step and the low solubility of MoO_3 in silica should thus lead to the migration of Mo species toward the surface. Surface characterization techniques attest that this approach was relevant. Indeed, a significant Mo-enrichment of the catalyst surface was observed after calcination. Moreover, the amounts of Mo detected by XPS at the surface and by TOF-SIMS at the outermost surface of the SG catalysts are very close to the amounts of Mo detected for WI samples. Considering that in the WI-samples Mo was deposited onto the surface of the silica−alumina support, these results suggest that a relatively high proportion of Mo species did migrate toward the surface of the sol−gel catalysts. It is noteworthy, however, that the Mo chemical environment appears to be different in WI and in SG samples, as underlined by the different position and width of the XPS Mo 3d peaks.

4.3. Nature of the Mo Species. It is usually accepted that for acting as a metathesis active center, Mo oxide should not be in its crystalline MoO_3 form.[32,33] Instead, more dispersed species are believed to be the precursors for the active species that form after activation. In our new preparation method, the dispersion of Mo species in

(31) Balikdjian, J. P.; Davidson, A.; Launay, S.; Eckert, H.; Che, M. *J. Phys. Chem. B* **2000**, *104*, 8931–8939.
(32) Topka, P.; Balcar, H.; Rathousky, J.; Zilkova, N.; Verpoort, F.; Cejka, J. *Microporous Mesoporous Mater.* **2006**, *96*, 44–54.
(33) Zhang, B.; Liu, N.; Lin, Q.; Jin, D. *J. Mol. Catal.* **1991**, *65*, 15–28.

the sol−gel samples appeared excellent. Virtually no bulk MoO_3 was detected by XRD in the SG catalysts even at 20 wt% MoO_3 loading, whereas in WI catalysts, the formation of crystalline molybdenum oxide could not be avoided already from MoO_3 loading as low as 8 wt%. This is a limitation of classical preparation methods, which induces an obvious constraint: overloading of Mo should be avoided to prevent detrimental effect of bulk MoO_3 on the specific activity. Our technique is perceived as very promising to overcome this limitation. Very interestingly, TOF-SIMS results provide strong indications that only isolated Mo species are present at the surface of SG catalysts. On the contrary, cluster ions containing more than one Mo atom are detected on WI samples. The occurrence of such species suggests the presence of agglomerated Mo oxide surface species (bulk crystals or polymeric species). In contrast, the nonhydrolytic sol−gel route produces highly dispersed, isolated Mo oxide species.

The activity measurements in the self-metathesis of propene can be understood in light of the aforementioned characterization results. The performances of WI catalysts reported in the present paper are consistent with other recent reports concerning Mo oxide-based catalysts. Expressed in terms of "turn over frequency" (TOF), namely, the number of propene molecules converted per atom of Mo present in the reactor each second, the activity of our systems ranges between 0.003 and 0.008 s^{-1}. Other authors report activities ranging from 0.002 to 0.010 s^{-1} for similar systems,[24,34] and activities up to 0.015 s^{-1} were reported using ordered mesoporous supports.[32,35] At low MoO_3 loading, the WI catalysts clearly performed better than SG catalysts. It can be put forward that even if Mo species do migrate toward the surface of the SG catalysts, part of the Mo species were still not accessible for taking part in the reaction. However, this downside of the SG preparation technique is minimized and finally outbalanced at higher MoO_3 loading. The specific activity of WI catalysts reaches a plateau when the loading is increased, which indicates that the number of active, well-spread Mo species does not increase. This can be correlated with the formation of MoO_3 crystallites, as observed by XRD experiments on WI samples. On the contrary, in SG samples, the specific activity increases continuously with the MoO_3 loading, which leads at high Mo loading to a sol−gel catalyst with significantly higher specific activity than the best wet-impregnation catalyst. As the specific surface area of SG and WI catalysts are similar, the superior activity of the SG catalyst at high loading can in turn be correlated with the high dispersion of Mo species at the surface of the SG catalysts, as revealed by XRD and TOF-SIMS techniques. In particular, TOF-SIMS experiments suggest that only isolated Mo species are present at the surface of SG catalysts.

Isolated Mo oxide species have already been proposed as the active metathesis sites[32,36−38] along with dimeric[39] and dispersed polymolybdates[32] and are here clearly identified as the precursors for the active metathesis centers in SG catalysts. In situ characterization of the activated catalysts would be needed to gather information on the nature of the actual metathesis active centers.[40]

5. Conclusion

In summary, we have demonstrated that the one-step reaction of low-cost chloride precursors with diisopropopyl ether, followed by drying and calcination provided a simple and effective nonhydrolytic sol−gel route to ternary Si−Al−Mo oxides with well-controlled compositions and textures. These Si−Al−Mo oxides exhibited high surface areas, large pore diameters, and significant surface acidity. They can be described as an amorphous silica−alumina matrix exhibiting dispersed Mo surface species. These systems outperform classical wet impregnated catalysts at high loading.

Acknowledgment. This work was initiated and supported by the ≪FAME≫ Network of Excellence of the EU sixth FP. The authors gratefully acknowledge the Université catholique de Louvain and the Fonds National de Recherche Scientifique (FNRS) in Belgium and the Ministère de l'Enseignement Supérieur et de la Recherche and the Centre National de la Recherche Scientifique (CNRS) in France for financial support. D.P.D. acknowledges the FNRS for its Research Fellow position. The involvements of Unité de catalyse et chimie des matériaux divisés in the ≪Inanomat≫ IUAP network sustained by the ≪Service public fédéral de programmation politique scientifique≫ (Belgium) and in the Cost Action D41 sustained by the European Science Foundation are also acknowledged. The authors thank the Belgian Funds for Collective Fundamental Research (FRFC) for the financial support for the acquisition of the TEM.

Supporting Information Available: Details on the preparation of the samples, complete description of the XPS and TOF-SIMS characterizations tools and detailed catalytic results (PDF). This material is available free of charge via the Internet at http://pubs.acs.org

(34) Handzlik, J.; Ogonowski, J.; Stoch, J.; Mikolajczyk, M.; Michorczyk, P. *Appl. Catal., A* **2006**, *312*, 213–219.
(35) Balcar, H.; Čejka, J. In *Metathesis Chemistry: From Nanostructure Design to Synthesis of Advanced Materials*; Karabulut, S., Imamoglu, Y., Dragutan, V., Eds.; Springer: New York, 2007; pp 151−166.
(36) Anpa, M.; Kondo, M.; Kubokawa, Y.; Louis, C.; Che, M. *J. Chem. Soc., Faraday Trans. 1* **1988**, *84*, 2771–2782.
(37) Fierro, J. L. G.; Mol, J. C. In *Metal Oxides: Chemistry and Applications*; Fierro, J. L. G., Ed.; Taylor & Francis: Boca Raton, FL, 2006; p 517.
(38) Ivin, K. J.; Mol, J. C. *Olefin Metathesis and Metathesis Polymerization*; Springer: London, 1997.
(39) Handzlik, J. *Surf. Sci.* **2007**, *601*, 2054–2065.
(40) Balcar, H.; Mishra, D.; Marceau, E.; Carrier, X.; Zilková, N.; Bastl, Z. *Appl. Catal., A* **2009**, *359*, 129–135.